DOI: 10.51790/2712-9942-2021-2-2-5

# MAXIMUM ENTROPY METHOD FOR TIME-SERIES DATA OBTAINED FROM REAL-TIME EVOLUTION OF TIME DEPENDENT DENSITY FUNCTIONAL THEORY

**Yasunari Zempo**[a], **Satoru S. Kano**[b]
*Hosei University, Tokyo, Japan*
[a] *ORCID: http://orcid.org/0000-0001-8760-8489, zempo@hosei.ac.jp*
[b] *ORCID: http://orcid.org/0000-0002-0081-0121, kano@ hosei.ac.jp*

*Abstract:* the maximum entropy method is one of the key techniques for spectral analysis. The main feature is to describe spectra in low frequency with short time-series data. We adopted the maximum entropy method to analyze the spectrum from the dipole moment obtained by the time-dependent density functional theory calculation in real time, which is intensively studied and applied to computing optical properties. In the maximum entropy method analysis, we proposed that we use the concatenated data set made from several-times repeated raw data together with the phase. We have applied this technique to spectral analysis of the dynamic dipole moment obtained from time-dependent density functional theory dipole moment of several molecules such as oligo-fluorene with $n = 8$. As a result, the higher resolution can be obtained without any peak shift due to the phase jump. The peak position is in good agreement to that of FT with just raw data. This paper presents the efficiency and characteristic features of this technique.

*Keywords*: spectrum analysis, time series data, maximum entropy method, time-evolution, time-dependent density functional theory.

*Acknowledgements*: the authors would like to express their gratitude to Professor H. Hanaizumi for useful discussions, and to Professor V. Savchenko for enthusiastic encouragements. This work was partially supported by JSPS Grants-in-Aid for Scientific Research (C) Grant number 16K05047, and Sumitomo Chemical, Co. Ltd.

*Cite this article*: Zempo Y., Kano S. S. Maximum Entropy Method for Time-Series Data Obtained from Real-Time Evolution of Time Dependent Density Functional Theory. *Russian Journal of Cybernetics*. 2021;2(2):64–73. DOI: 10.51790/2712-9942-2021-2-2-5.

# ПРИМЕНЕНИЕ МЕТОДА МАКСИМАЛЬНОЙ ЭНТРОПИИ К ВРЕМЕННЫМ РЯДАМ, ПОЛУЧАЕМЫМ В РЕАЛЬНОМ ВРЕМЕНИ В РАМКАХ НЕСТАЦИОНАРНОЙ ТЕОРИИ ФУНКЦИОНАЛА ПЛОТНОСТИ

**Я. Земпо**[а], **С. С. Кано**[б]
*Университет Хосэй, Токио, Япония*
[а] *ORCID: http://orcid.org/0000-0001-0760-8489, zempo@hosei.ac.jp*
[б] *ORCID: http://orcid.org/0000-0002-0081-0121, kano@hosei.ac.jp*

*Аннотация:* метод максимальной энтропии — один из основных в спектральном анализе. Его главная особенность — описание низкочастотных спектров короткими временными рядами данных. Авторы применили метод максимальной энтропии для анализа спектров дипольного момента, полученных расчетами в реальном времени по нестационарной теории функционала плотности. Данный вопрос интенсивно изучается и находит практическое применение при расчетах оптических свойств. При анализе методом максимальной энтропии предложено использовать объединенные наборы данных, включающие несколько повторяющихся последовательностей исходных данных с учетом фазы. Данный метод был применен при проведении спектрального анализа динамического дипольного момента, рассчитанного по нестационарной теории функционала плотности на основе дипольного момента нескольких молекул — в частности, молекул олигофлуорена при $n = 8$. В итоге удалось повысить разрешение без смещения максимумов из-за скачка фазы. Положение максимумов хорошо согласуется с результатами применения преобразования Фурье к необработанным исходным данным. В настоящей статье представлены особенности данного метода и показатели его эффективности.

*Ключевые слова*: спектральный анализ, временные ряды данных, метод максимальной энтропии, развитие во времени, нестационарная теория функционала плотности.

*Благодарности*: авторы выражают благодарность проф. Х. Ханаизуми (H. Hanaizumi) за полезные обсуждения и проф. В. Савченко за всемерную поддержку исследования. Работа частично поддержана субсидией на научные исследования № 16K05047, предоставленной Японским обществом развития науки (JSPS), а также компанией Sumitomo Chemical, Co. Ltd.

*Для цитирования*: Земпо Я., Кано С. С. Применение метода максимальной энтропии к временным рядам, получаемым в реальном времени в рамках нестационарной теории функционала плотности. *Успехи кибернетики*. 2021;2(2):64–73. DOI: 10.51790/2712-9942-2021-2-2-5.

## Introduction

The maximum entropy method (MEM) is frequently used to analyze natural phenomena with long periods such as earth and planetary science, and seismic waves and tsunamis that can be measured for a short time [1]. However, little research has been done on applying MEM to the optical spectrum analysis associated with the electronic structure calculation. The purpose of the research is to apply this method to electronic state calculation.

Time-dependent density functional theory (TDDFT) is one of the most prominent and widely used tool for calculating excited states. A real-time and real-space technique is employed to solve the time-dependent Kohn-Sham equations. Within the framework of this approach, the wave functions are calculated by the finite difference method on real spatial grids [2, 3] without using explicit bases such as plane waves or Gaussian. In our procedure to calculate optical properties, we use the time-series data, namely the dynamic dipole moment. In a usual technique, Fourier transform (FT) is applied to it for calculating optical properties to derive the electronic transition spectrum from TDDFT. The most useful information is obtained in the low frequency region. Since the spectral resolution depends on the total time length of the dipole moment, to obtain the good resolution, the computational cost becomes quite expensive.

To solve this difficulty, we focus on Maximum Entropy Method (MEM) [4] which is one of the key techniques of spectrum analysis. MEM is based on the of the information theory for estimating unknown probability distributions relevant to the information about their expected values. The main feature is to obtain a fairy high resolution and accuracy with a relatively small number of time-series data. This technique was applied to the spectral analysis of time-dependent dipole moments of molecules, which is calculated by real-time TDDFT, and evaluated the efficiency of this method. We realize that MEM needs less time step than FT to obtain the optical spectrum with same level resolution [5]. Further, we proposed to use the concatenated data set made from several-times repeated raw data [6] together with the phase to minimize the side effect of the artificial periodicity. The introduction of this MEM provides the much better spectral resolution of the target peak near the energy gap.

The paper is organized as follows. In the next section, we briefly describe a procedure of our TDDFT calculation. Then, we explain MEM and our signal enhancement technique. In following section, we present our results of absorption spectra of some molecules, discuss the efficiency, and finally summarize our techniques.

## Time-Series Data Obtained from Real-Time Evolution

The essential in recent development of material depends on the density functional theory, which is based on the ground state, and successfully in describing the physical properties of materials. On the other hand, in describing the optical responses and the excitation spectra where the electronic excited states are involved, DFT is much less successful. However, this difficulty is, in principle, solved by the extension of DFT to time-dependence, e.g., TDDFT, which was established by Runge and Gross [7]. In analogy to the time-independent case, the TDDFT equation of motion coupled with pseudopotentials is given by

$$H\psi_k(\boldsymbol{r},t) = i\frac{\partial}{\partial t}\psi_k(\boldsymbol{r},t)\,, \tag{1}$$

$$H = -\frac{1}{2}\boldsymbol{\nabla}^2 + V_{ps}(\boldsymbol{r},t) + V_H(\boldsymbol{r},t) + V_{XC}(\rho(\boldsymbol{r},t)) + V_{ext}(\boldsymbol{r},t)\,, \tag{2}$$

where $V_{ps}$ ion is an ionic pseudopotential, $V_H$ is the Hartree potential, and $V_{XC}$ is the exchange-correlation potential. Since the exact time-dependent xc kernel is not known, the originally nonlocal time-dependent xc kernel is replaced with a time-independent local one. This is reasonable when the density varies slowly with time. This approximation allows the use of a standard local ground-state xc functional in the TDDFT frame work. The Hartree and exchange-correlation potentials can be determined from the electronic charge density, $\rho(\boldsymbol{r},\mathrm{t}) = \sum_j \left|\psi_j(\boldsymbol{r},t)\right|^2$. The summation is over all occupied states $j$. The Hartree potential is determined by $\nabla^2 V_H = -4\pi\rho$, and as the xc potential $V_{XC}$, the usual local density approximation (LDA) is used in our study. For the ionic potential, we employ the pseudopotential $V_{ps}$ in the separable form so that the only valence electrons are considered. Prior to the calculation of optical responses, we first obtain the optimized electronic structure. Then, we apply an external field $V_{ext} = -k\delta(t)\,z$ to the system as a perturbation and follow the linear responses of the system in real time. The time dependent wave function is given by $\psi(t) = \exp[-iHt]\ \psi(0)$, with the initial wave function $\widetilde{\psi}$ at $t = 0$, $\widetilde{\psi}|_{t=0} = e^{ikz}\psi(0)$, where $H$ is the Hamiltonian of the system, and $k$ is a small wave number corresponding to the external perturbation in the $z$ direction.

$$\mu(t) = \sum\nolimits_i \langle\psi_i(\boldsymbol{r},t)|\boldsymbol{r}|\ \psi_i(\boldsymbol{r},t)\rangle \tag{3}$$

The polarizability $\alpha(\omega)$ is numerically calculated using the fast Fourier transformation (FT) of $\mu(t)$ as follows.

$$\alpha(\omega) = \frac{1}{k}\int dt\exp\left[-i\omega t\right]\ \mu(t) \tag{4}$$

The oscillator strength $S(\omega)$ is related to the imaginary part of the polarizability,

$$S(\omega) = \frac{2\omega}{\pi}\mathrm{Im}\ \alpha(\omega)\,. \tag{5}$$

In our approach, we use MEM in this procedure in eq. (4) and (5), considering the dynamic dipole moment $\mu(t)$ as a time series data. Figure 1 shows the dynamic dipole moment of benzene.

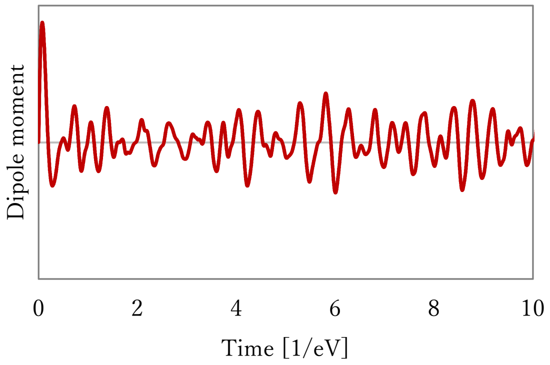

**Figure 1.** *Example of dynamic dipole moment of benzene*

Although this type of TDDFT is simple calculation, e.g., time-evolution of the ground state due to the external potential at $t = 0$, the effect is quite significant. Figure 2 shows the HOMO-LUMO gap of benzene, compared this TDDFT to the results from the usual density functional theory (DFT) with the local density approximation (LDA), the generalized gradient approximation (GGA), and the experiment. The simple LDA provides a small gap 5.04 eV. When we use GGA, the gap is slitely improved. TDDFT calculation give us the value 6.90 eV, which is comparable to the experimantal value 6.94 eV.

### Maxmum Entropy Method

As shown in the previous section, the resolution of the FT absorption spectrum $S(\omega)$ is $\sim T^{-1}$, corresponding to the finite spectral bandwidth of the limited time series of $\mu(t)$, where $T = N\Delta t$ is the total evolution time. MEM, in contrast, estimates the full spectrum from the limited data based on information theory. The entropy in information theory has been recognized as a measure of uncertainty [8-10]. Any inferences made from incomplete information should use with the probability distribution which maximizes the entropy under the constraints of available information [11]. The present study is based on Burg's method

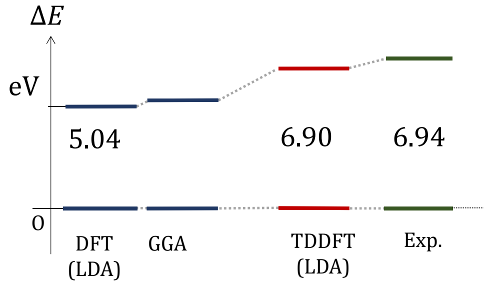

**Figure 2.** *Comparison of the benzene band gap calculated by LDA, GGA, TDDFT that are referenced to experimental data*

[12], where the dipole moment $\mu$ is assumed to be a random variable and the samples are given by TDDFT, $\mu_m{=}\mu(m\varDelta t)$. The calculated autocorrelation $C_m$ at the time lag $m$ is

$$C_m = \frac{1}{N-|m|} \sum_{n=0}^{N-|m|-1} \mu_n^* \mu_{n+|m|}. \tag{6}$$

In Eq. (6), we use the general autocorrelation form in the case of the general time-series data. For $N \to\infty$, the Fourier transformation of the autocorrelation function is the power spectrum $P\,(\omega)$ [13] which is directly comparable to $S(\omega)$.

$$P\,(\omega)/\varDelta t = \sum_{m=0}^{\infty} C_m \exp(-i\omega m \Delta t) \tag{7}$$

$$C_m = \frac{1}{2\pi} \int_{-\pi/\Delta t}^{\pi/\Delta t} P\,(\omega) \exp(i\omega m \Delta t)\ d\omega \tag{8}$$

When each random variable $\mu_n$ obeys the Gaussian distribution,

$$h \ \propto \int_{-\frac{\pi}{\varDelta t}}^{\frac{\pi}{\varDelta t}} \log P\,(\omega) \ \ d\omega \tag{9}$$

is maximized, and thus $h$ is taken as the entropy. Conversely, under the constraints of Eq. (6) with the given value of Eq. (4), we find the value $\hat{P}\,(\omega)$ which maximizes Eq. (7). The solution is

$$\hat{P}\,(\omega)/\varDelta t = \left| \frac{\beta}{1+\sum_{k=1}^{M} a_k \exp\,(ik\omega\Delta t)} \right|^2, \tag{10}$$

where $M(\leq N)$ is the maximum number of $|m|$ in Eq. (4). The parameters $a_k$ are the Lagrange multipliers which are the solution of the Yule-Walker equation

$$C_m = \sum_{k=1}^{M} a_k C_{m-k} + |\beta|^2 \delta_{m,0}, \tag{11}$$

or equivalently, the linear Toeplitz matrix equation [13],

$$\begin{pmatrix} C_0 & C_1 & \cdots & C_M \\ C_1 & C_0 & \cdots & C_{M-1} \\ \vdots & \vdots & & \vdots \\ C_M & C_{M-1} & \cdots & C_0 \end{pmatrix} \begin{pmatrix} 1 \\ a_1 \\ \vdots \\ a_M \end{pmatrix} = \begin{pmatrix} |\beta|^2 \\ 0 \\ \vdots \\ 0 \end{pmatrix}. \tag{12}$$

We adopt the Levinson-Durbin algorithm to solve Eq. (3) efficiently. The Yule-Walker equation Eq. (9) is also derived by the autoregressive model. We also extend the autocorrelation to the complex data, which is useful and explained in detail in the next section.

The periodicity of the signal is expressed by the lag in the autocorrelation. Figure 3($a$) shows the relation of periodicity and the lag $m$ schematically. The value at shorter lags shows the contribution from high frequencies, and the value at longer lags shows the contribution from low frequencies. Even though the information in the low energy region is important for the optical spectrum analysis, the value of the autocorrelation at larger lags can become quite small. In the autocorrelation calculation, the maximum size lag $m$ is denoted by $M$ Of course, the effective value of $M$ is restricted by the number of data $N$. Therefore, we require a sufficiently large $N$ to obtain a reasonable spectral resolution in the low frequency region; the same as in the case of FT.

### Signal Enhancement Technique

As a new MEM, we propose using a concatenated data set made from repeated raw data coupled with the phase shift so as to minimize the side effect of artificial periodicity. Our interests are in the in the lower energy region such as the energy gap. To emphasize the signal in this region, we need a larger lag $M$, which is the maximum lag of the autocorrelation. However, increasing $M$ sometimes causes unphysical results such as peak splits and false peaks. In addition, the number $M$ is limited by the total number of time steps $N$. To solve this difficulty, we repeat the raw data many times as shown in Fig. 3($b$). The resolution in the lower energy region is attributed to the maximum lag $M$. With the repeated signal, the value of $M$ may be selected at sufficiently large values without additional computations. With this procedure, we can save on computational costs.

At the concatenated point, of course, there is a phase jump for each frequency component, which is recognized as noise in the total signal. The side effect of phase jump may be added, for example, the peak shifts. To reduce side effects of the phase jump such as peak shifts, we introduced a phase shift at each concatenated data in the repeated data.

$$\mu(n) = \mu'(n)\exp(ik\phi) \ , \tag{13}$$

where $\mu'(n)$ is the repeated raw data, and $\widehat{\mu}(n)$ is the $k$-times repeated and concatenated data $\mu'(n)$ with an appropriate phase $\phi$ for the target frequency ($-\pi \leq \phi \leq \pi$). This introduction of the phase to the signal does not affect to the total power spectrum due to the definition used in Eq. (8). Of course, a different target frequency has a different phase. Since the phase $\phi$ is a constant value, it is necessary to choose the appropriate phase for the target frequency to minimize the side effects of the phase jump due to the concatenated repeated data.

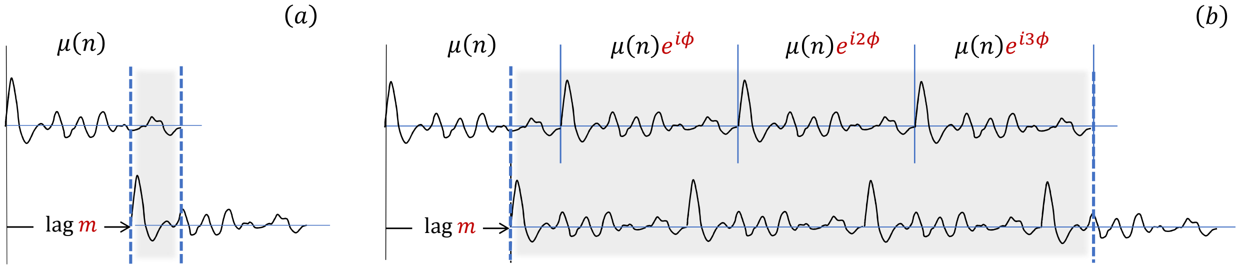

**Figure 3.** *Conceptual image of the autocorrelation calculation for* ($a$) *the raw data, and* ($b$) *our concatenated data made from several-times repeated raw data together with the phase*

Figure 4. shows the practical dynamic dipole moment $\widehat{\mu}(n)$ that the three times concatenated data $N = 5000$, and the maximum lag $M = 1800$ with the phase shift $\phi = -0.25\pi$. Although this dipole moment is complex, we can calculate the autocorrelation using Eq. (6). The Yule-Walker equation does not change, and we solve eq. (12) as usual. The calculated spectrum $S(E)$ by our MEM method is shown in Fig. 5. In this case, the target peak or the lowest energy peak is the first peak around 7.5eV, which is shown as an arrow in Fig. 5($a$). In Fig. 5, we compare the spectrum $S(E)$ obtained from the non-repeated data $N = 5000$, and the concatenated data $N = 5000 \times 100$ together with an appropriate phase $\phi = -0.25\pi$, and that concatenated data in out of phase $\phi = \pi$. In all cases, we use the maximum lag $M$= 1800. For the benzene molecule, this time step seemingly provides a good resolution so as to see the first peak clearly.

However, there are differences due to the side effect of phase jump as mentioned above. In Fig. 5($b$), the first peak in detail is described in the region from 6.5 eV to 7.5 eV. Our method with the matched phase provides the good resolution compared with that of a conventional MEM. On the other hand, the result of the mismatched phase provides the different peak position and the broad peak. To obtain a good spectrum, corresponding to the energy gap peak, we have to find the matched phase. If we choose the mismatched phase for the target peak, the position of that peak shifts, and the strength decreases. From this point of view, we can select the better phase both to make the target peak sharp and to maximize the strength.

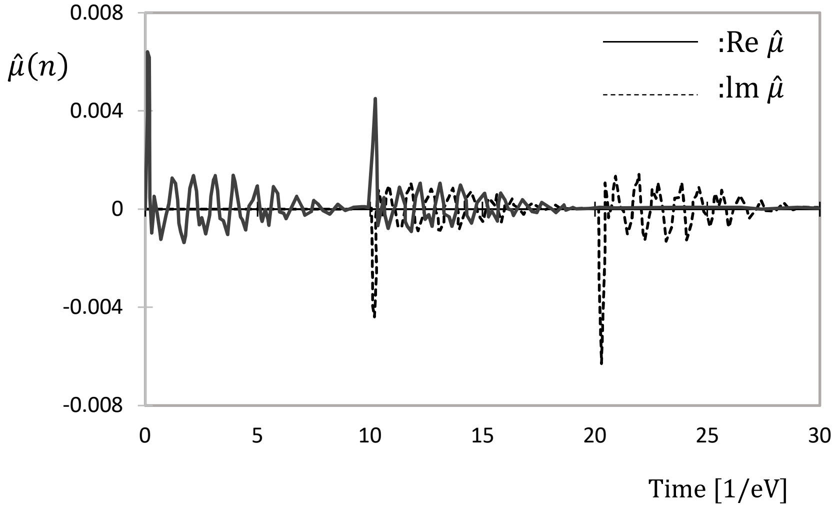

**Figure 4.** *The Concatenated repeated raw data* $N = 5000 \times 3$*, and* $M = 1800$ *of Benzene dipole moment together with the phase* $\phi = -0.25\pi$*. The solid and the dotted line shows the real and imaginary part, respectively*

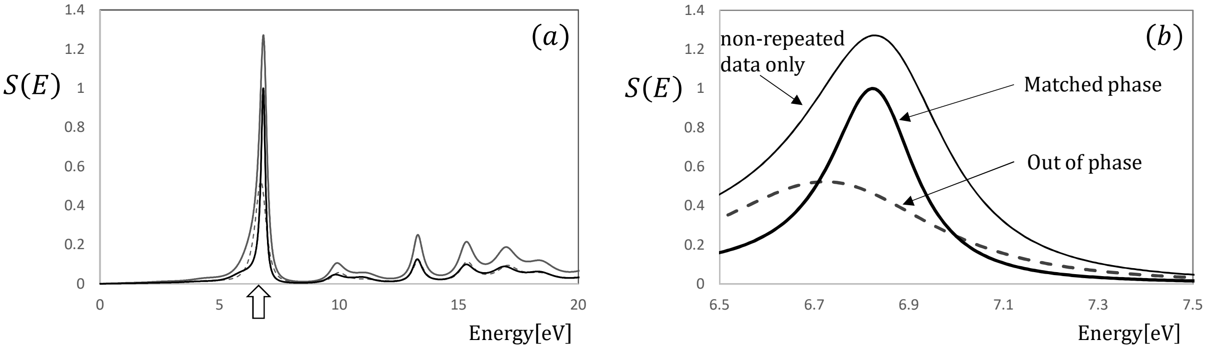

**Figure 5.** *Comparison of the spectrum each condition: Thin solid line shows the MEM spectrum with non-repeated data* $N = 5000$*; Thick line shows the spectrum with the repeated data* $N = 5000 \times 100$ *and matched phase,* $\phi = -0.25\pi$*; Dotted line is the spectrum with the repeated data* $N = 5000 \times 100$ *and out of phase* $\phi = \pi$

Our method with the matched phase provides the good resolution compared with that of a conventional MEM. On the other hand, the result of the mismatched phase provides the different peak position and the broad peak. To obtain a good spectrum, corresponding to the band gap peak, we have to find the matched phase. Spectrum our MEM comparison obtained from the time-series data for benzene, which was made using real-time TDDFT. (a) Real time evolution up to $N = 20000$ for FT. (b) Four times repeated data of the dipole moment with $N = 5000 \times 4$. (c) The data in panel (b) together with the phase $\phi = 0.25\pi$. The solid line is the real part of the data, and the dashed line is the imaginary part of the data.

### Results for small and mediumsize molecules

As a simple example to confirm the efficiency of our proposed method, we applied our MEM to the analysis of benzene, naphthalene, anthracene, and tetracene. The molecular structure of these molecules is based on the ground state. The time evolution is carried out according to real-time TDDFT [14]. The spectrum $S(\omega)$ is calculated from the time-series data in our MEM technique. The results are shown in Fig. 6, where the solid line is meant for the result for benzene, the dashed line is that for naphthalene, the dash-dotted line is that for anthracene, and the dotted line is that for tetracene. These spectra are normalized by the intensity at the first peak. Figure 6($a$) shows the results of the improved MEM. The parameters ($M$ and $\phi$) of our MEM are $M = 1800$ and $\phi = -0.25\pi$ for the analysis of benzene, $M = 2500$ and $\phi = -0.20\pi$ for that of naphthalene, $M = 2000$ and $\phi = -0.23\pi$ for that of anthracene, and $M = 3000$ and $\phi = -0.21\pi$ for that of tetracene. For both MEM calculations, the same number of the time steps, $N = 10000\times 100$, is used. Figure 6($b$) shows the results of FT with $N = 10000$. Our method provides good resolution compared with that of FT. In addition, we can see a clear spectrum in comparison to FT. This is one feature of our MEM.

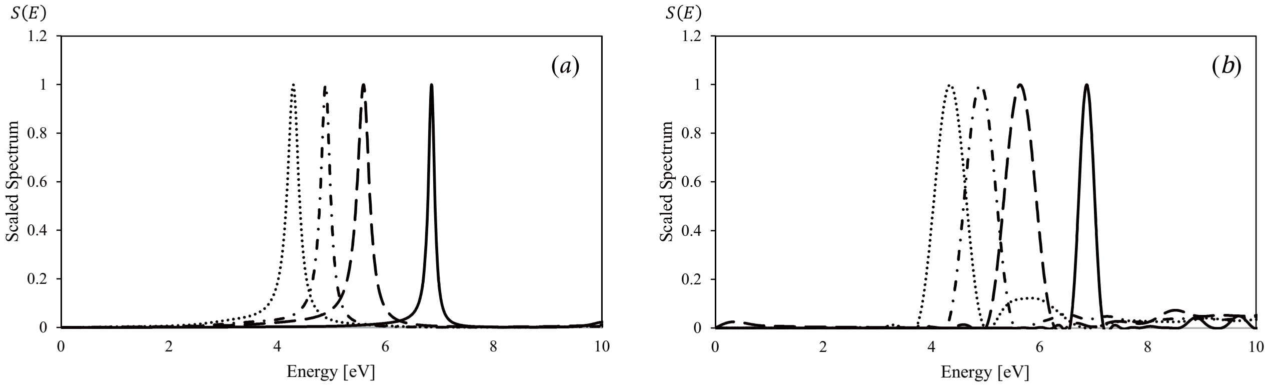

**Figure 6.** *Comparison of the improved MEM and FT spectra for benzene (solid line), naphthalene (dashed line), anthracene (dash-dotted line) and tetracene (dotted line).* ($a$) *Results of our MEM using* $N = 10000 \times 100$ *with* ($M = 1800, \phi = -0.25\pi$), *for benzene,* ($M = 2500, \phi = -0.20\pi$), *for naphthalene,* ($M = 2000, \phi = -0.23\pi$) *for anthracene, and* ($M = 3000, \phi = -0.21\pi$) *for tetracene.* ($b$) *Results of FT with* $N = 10000$. *All the spectra are normalized at the first low energy peak*

Poly(9,9-dialkyl-uorene) and their substituted derivatives are used as organic LED material and are expected to be basic materials for blue emission LEDs. Their electronic structures have been extensively studied [15]. We employed the oligomer of fluorene (oligo-FL) with $n = 8$ and performed the MEM calculation. The molecule size is fairly large; therefore, then the calculation for each step is quite expensive. It takes a long time to perform the calculation to obtain the low energy part of the spectrum. If we can save on the calculation cost when calculating the lower energy part of the spectrum, our method will be considered effective. We applied our MEM to this signal analysis. Figure 7 shows a comparison of the absorption spectra using four different methods. The solid line shows the result of our MEM with $N = 5000\times 100$, $M = 2500$ and $\phi = 0.25\pi$ the dashed line is that of FT for $N = 20000$, the dash-dotted line is our conventional MEM spectrum with just the real time steps $N = 5000$ and $M = 2500$, and the dotted line is that of MEM with $N = 5000 \times 100$ and $M = 2500$. These spectra are normalized at the second low energy peak, which is relevant to the absorption of a fluorene unit.

FT (the dashed line) and the simple MEM (the dash-dotted line) provide a broad peak at the bandgap area. With only the repeated signal (the solid and dashed lines), the strength of the first peak is emphasized. Without a phase shift, we can observe that the peak position shifts due to the side effect of the phase jump [6]. However, we can obtain a clear first peak using our new method (the solid line). In this case, we choose the matched phase corresponding to the first peak. Therefore, the position of the second peak differs from those in the other methods. (Note that the normalization of the signal was done at the second peak.) If we choose the mismatched phase for the target peak, the position of the peak shifts and the strength, decreases as we mentioned above. The bandgap peak at 2.53 eV for our MEM may correspond to the experimentally observed peak at 3.56 eV for poly-FL. This discrepancy is due to an inherent problem in DFT.

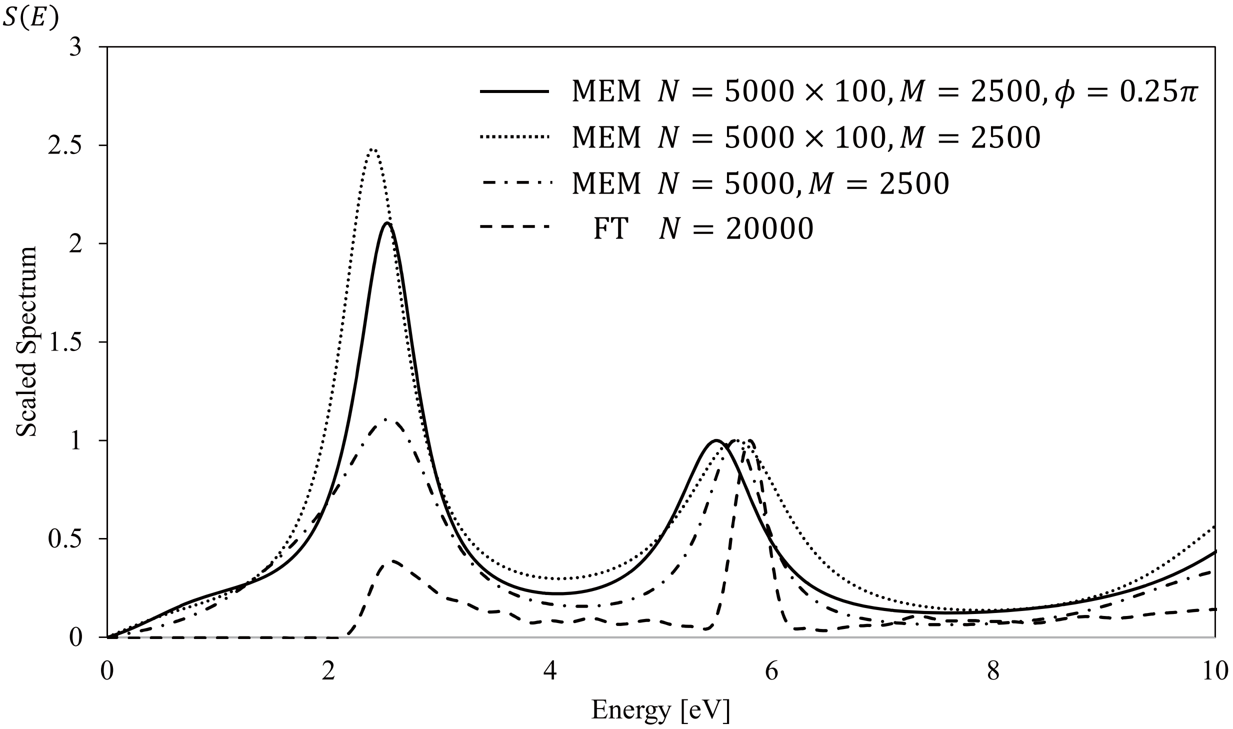

**Figure 7.** *Comparison of the absorption spectrum for oligo-fluorene with* n$=8$. *The dashed line is the result of FT with* $N = 20000$*, the dash-dot line is that of MEM with* $N = 5000$*, the dotted line is the that of MEM with repeated data* $N = 5000 \times 100$*, and the solid line is that of our MEM with* $N = 5000 \times 100$*,* $M = 2500$ *and* $\phi = 0.25\pi$*. Spectra are normalized at the second low energy peak*

## Discussions

In our MEM, there are two important issues. One is the use of a concatenated data set made from repeated raw data. The other is the introduction of the phase to minimize the artificial periodicity. In MEM, the periodicity is on the autocorrelation function. The small lag $m$ and large lag m represent information of higher and lower frequencies, respectively. If we have infinite time-series data, there is no difference between the signal strength in high and low frequency. However, we have is finite time-series data. Naturally, the information of the lower frequencies decreases compared to that of the higher frequencies. The interests are, on the other hand, in the low energy region such as energy gaps in the optical material properties.

Figure 8 shows the magnitude of the Yule-Walker equation eq. (12). In the traditional MEM, the magnitude of the diagonal element is the largest. Then, that of the off diagonal elements decreases as shown in Fig. 8($a$). When we use the concatenated made from repeated raw data, we can see the higher-order autocorrelation functions (around the upper right and lower left corners of the matrix) clearly contain a lot of long-period information as expressed in Fig. 8($b$).

The selection of the appropriate phase is depend on the target peak. As we see the spectrum in Fig. 7. In our MEM ($N = 5000 \times 100$) using just repeated data, the intensity of the first peak is the most developed. However, the peak position is shifted. On the other hand, in our proposed method ($N = 5000 \times 100$, and $\phi = 0.25\pi$), there is no deviation in the position of the first peak, and we can obtain the good resolution. Although the intensity is different, it is a sharper developed peak than the FT of $N = 20000$. In Fig. 7, the phase $\phi$ was decided for the largest first peak. Naturally, the value of $\phi$ is different at the second peak. If an inappropriate $\phi$ is used in this calculation, the peak will be out of position, and the intensity will decrease. Good example is the spectrum around the second peak. The intensities of the second peak are normalized for all cases. We can see that only the second peak position has changed, because the phase was selected for the first peak.

In addition, our MEM is not always work well for target peak. With this method for the spectrum analysis, we cannot obtain the low energy component which is not included in the data. We have to calculate a certain level of the time evolution until the information of the low energy part is obtained.

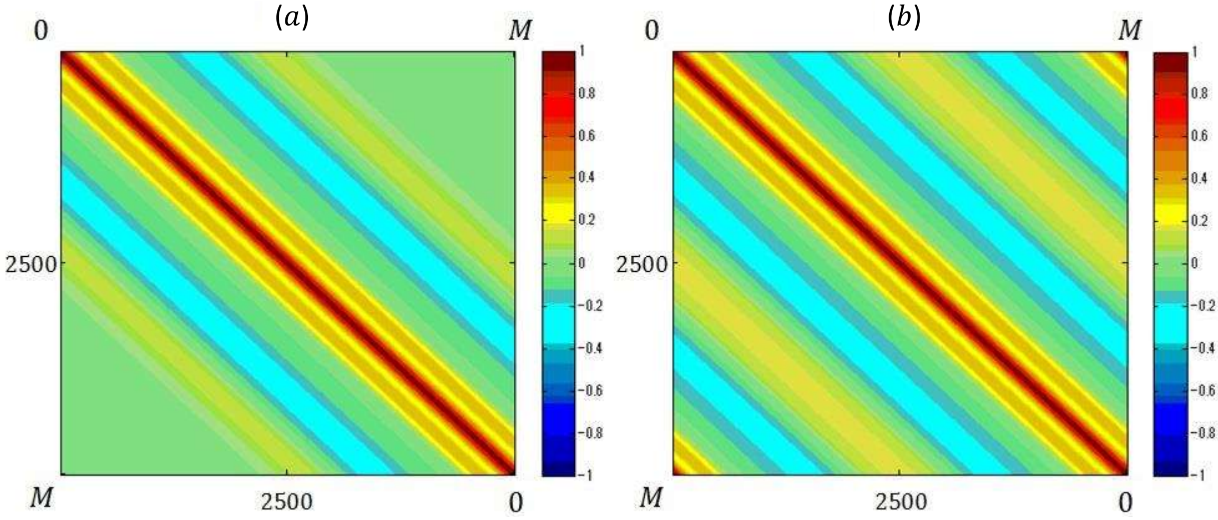

**Figure 8.** *The effect of repeated data on long-period components. The magnitude of each matrix elements of the coefficient matrix in eq.* (12) *is represented by a color distribution.* (*a*) *The results of* $N = 5000$, *and* (*b*) *the results of* $N = 5000 \times 100$ *are shown. In both cases,* $M = 4999$. *All elements are normalized by the diagonal element value (autocorrelation function with lag* 0, $C_0$*), which is expressed as dark red*

### Summary

We employed MEM to obtain optical spectra of molecules, and the spectral resolution was quite improved, which is better than that of FT with the same number or total time steps. As a new aspect, we introduced the use of repeated the same signal together with the phase to make apparently long data. The resolution of the spectrum is dependent on the total number of time steps $N$ and the autocorrelation lag $M$. A longer time lag is involved, the spectrum is efficiently enhanced in the lower frequency region. We obtained quite better resolutions for target peak without adding practical machine time. This means that we can save our calculation cost efficiently.

## REFERENCES

1. Sakurai T. Eleven-Year Solar Cycle Periodicity in Sky Brightness Observed at Norikura, Japan. *Earth Planets Space.* 2002;54(2):153–157. DOI: 10.1186/BF03351715.
2. Chelikowsky J. R., Troullier N., Wu K., Saad Y. Higher-Order Finite-Difference Pseudopotential Method: an Application to Diatomic Molecules. *Physical Review B.* 1994;50(16):11355–11364. DOI: 10.1103/PhysRevB.50.11355.
3. Yabana K., Bertisch G. F. Time-Dependent Local-Density Approximation in Real Time. *Physical Review B.* 1996;54(7):4484–4487. DOI: 10.1103/PhysRevB.54.4484.
4. Burg J. P. A New Analysis Technique for Time Series Data. NATO Advanced Study Institute on Signal Processing. 1968;15-0. Enschede, Netherlands.
5. Toogoshi M., Kato M., Kano S. S., Zempo Y. Optical Spectrum Analysis of Real-Time TDDFT Using the Maximum Entropy Method. *Journal of Physics: Conference Series.* 2014;510:012027. DOI: 10.1088/1742-6596/510/1/012027.
6. Toogoshi M., Kano S., Zempo Y. Improved Maximum Entropy Method applied to Real-Time Time-Dependent Density Functional Theory. *Journal of Physics: Conference Series.* 2017;905:012006. DOI: 10.1088/1742-6596/905/1/012006.
7. Runge E., Gross E. K. U. Density-Functional Theory for Time-Dependent Systems. *Physical Review Letters.* 1984;52(12):997–1000. DOI: 10.1103/PhysRevLett.52.997.
8. Shannon C. E. A Mathematical Theory of Communication. *The Bell System Technical Journal.* 1948;27(3):379–423. DOI: 10.1002/j.1538-7305.1948.tb01338.x.
9. Shannon C. E. A Mathematical Theory of Communication. *The Bell System Technical Journal.* 1948;27(4):623–656. DOI: 10.1002/j.1538-7305.1948.tb00917.x.

10. Jaynes E. T. Information Theory and Statistical Mechanics. *Physical Review*. 1957:106(4);620–630. DOI: 10.1103/PhysRev.106.620.
11. Jaynes E. T. On the Rationale of Maximum-Entropy Methods. *Proceedings of the IEEE*. 1982;70(9):939–952. DOI: 10.1109/PROC.1982.12425.
12. Haykin S., Kesler S. Prediction-Error Filtering and Maximum-Entropy Spectral Estimation. Haykin S. (eds) *Nonlinear Methods of Spectral Analysis. Topics in Applied Physics.* 1979;34:9–72. Springer, Berlin, Heidelberg. DOI: 10.1007/3-540-12386-5_9.
13. Kauppinen J. K., Maffat D. F., Hollberg M. R., Mantch H. A. New Line-Narrowing Procedure Based on Fourier Self-Deconvolution, Maximum Entropy, and Linear Prediction. *Applied Spectroscopy*. 1991;45(3):411–416. DOI: 10.1366/0003702914337155.
14. Zempo Y., Akino., Ishida M., Ishitobi M., Kurita Y. Optical Properties in Conjugated Polymers. *Journal of Physics: Condensed Matter*. 2008;20(6):064231. DOI: 10.1088/0953-8984/20/6/064231.
15. Hummer K., Puschnig P., Sagmeister S., Ambrosch-Draxl C. Ab-Inito Study on the Excitation Binding Energies in Organic Semiconductors. *Modern Physics Letters B*. 2006;20(6):261–280. DOI: 10.1142/S0217984906010603.